The Determination of Multiple Steady States in Two Families of Biological Systems

Guo-Syong Chuang, Pang-Yen Ho, and Hsing-Ya Li

Department of Chemical Engineering, National United University, Miaoli, Taiwan, 36003 R. O. C.

Reprint requests to G.-S. Ch.; Fax: +886-37-332397, E-mail: chuang@nuu.edu.tw

Z. Naturforsch. **59a,** 136 – 146 (2004); received December 20, 2003

The capacity of computational multiple steady states in two biological systems are determined by the Deficiency One Algorithm and the Subnetwork Analysis. One is a bacterial glycolysis model involving the generation of ATP, and the other one is an active membrane transport model, which is performed by pump proteins coupled to a source of metabolic energy. Mass action kinetics, is assumed and both models consist of eight coupled non-linear equations. A set of rate constants and two corresponding steady states are computed. The phenomena of bistability and hysteresis are discussed. The bifurcation of multiple steady states is also displayed. A signature of multiplicity is derived, which can be applied to mechanism identifications if steady state concentrations for some species are measured. The capacity of steady state multiplicity is extended to their families of reaction networks.

Key words: Multiple Steady States; Glycolysis; Active Membrane Transport; Bistability; Hysteresis; Bifurcation

1. Introduction

Some exotic dynamic phenomena in isothermal chemical systems, such as unstable steady states, undamped oscillations and multiple steady states, have been shown experimentally [1 – 4]. This indicates that instabilities derive from the intricacy of chemistry itself, instead of from thermal effects for non-isothermal systems. In biotechnological applications, appearance of multiple steady states could lead to undesirable situations for bioprocess operation. It is important for the chemical engineer to be able to identify chemical systems that have the capacity to exhibit multiple steady states, since such an identification helps to design more efficient and safer reactors.

Biological cell systems, which usually consist of many species and reactions, can also give rise to those complex reaction behaviors [5 – 7]. One example studied in this work is a bacterial glycolysis system. Bacteria, like all other living cells, require certain nutrients such as glucose for growth. Although the cytoplasmic membrane of bacterial cells, such as *Escherichia coli and Bacillus subtilis*, is not easily permeable to glucose, it "picks up" glucose at the medium side of the membrane and releases it on cytoplasm side of the membrane. This transport is coupled to a chemical conversion of substrate, *i.e.*, the phosphorylation of glucose to glucose-6-phosphate [8]. A rudimentary description of glycolysis, a process by which a carbon source is digested by a cell, is formulated based upon pathways pertinent to bacteria [9]. Considering rate expressions of minimal complexity of three coupled equations, which do not include some important coupling and non-linearity present in bacterial glycolysis, Hatzimanikatis and Bailey [9] demonstrated that, for certain values of the system parameters, as many as ten steady states can be achieved.

The other example studied in this work is an active membrane transport system. The active transport is an important path to self-regulation and self-control in living cells. It is performed by pump proteins coupled to a source of metabolic energy, usually ATP hydrolysis. The transport is accomplished by a conformational change of the pump in transferring the solute across the membrane. This process can be modeled by specific kinetic steps for the binding and conformational changes, which are similar to those occurring in standard chemical kinetics. Some theoretical and experimental studies on this field have been done [10, 11]. Based on some experimental results [12, 13], Vieira and Bisch [14] have recently proposed a model (the model 5) with monomers as pump units. They have ap-

0932–0784 / 04 / 0300–0136 $ 06.00

plied stoichiometric network analysis [15] to study the stability of steady states and have numerically found a set of rate constants showing steady state multiplicity.

Recently, Li [16] has developed a Subnetwork Analysis for the determination of multiple steady states in isothermal, complex, chemical reaction networks. In the present work, the analysis is applied to show the capacity of multiple steady states in the two biological systems mentioned above. Although the possibility of steady state multiplicity was already shown by other researchers, there are some differences between this work and the other articles. The analysis methods used are different. The bacterial glycolysis model, simplified by Hatzimanikatis and Bailey [9], consists of only three coupled equations. In this work we study a more complex system, which consists of eight coupled non-linear equations. For both examples we determine not only the multiplicity of the model itself, the result is also extended to their family members. Moreover, a signature of multiplicity is derived, which can be used to identify the reaction mechanism. This work demonstrates a potential application of the Subnetwork Analysis to determine multiple steady states admitting complex biological reacting systems.

2. Theoretical Background

2.1. Reaction Networks and Mass Action Differential Equations

Example 1. Bacterial glycolysis model

The bacterial glycolysis model simplified by Hatzimanikatis and Bailey [9] arises from participation of ATP and ADP and from the involvement of PEP (phosphoenolpyruvate) in the glycolysis pathway. The overall reaction is Glucose + 2ADT → 2Pyruvate + 2ATP, which contains the following elementary steps:

$$\begin{array}{ll} S+E \to G+P, & S+T \to G+D, \\ G+T \to F+D, & F+2D \rightleftarrows 2E+2T, \\ E+D \to P+T, & M+T \rightleftarrows 2D, \\ D \rightleftarrows T, & \end{array} \tag{1}$$

where S and P correspond to extracellular glucose and pyruvate, G to the pool of glucose 6-phosphate and fructose 6-phosphate, F to fructose 1,6-diphosphate, E to phosphoenolpyruvate, M to AMP, D to ADP, and T to ATP.

The assumptions used in this work are: 1. the reactants, glucose and AMP, can diffuse into the reaction region inside of a cell; 2. the remaining reactants, glucose and AMP, and the product, pyruvate, keep diffusing out of the reaction system; 3. the enzyme activities depend only on the concentrations of their substrates and the cell is not growing; 4. the elementary steps in (1) are all reversible; 5. the reaction system is well mixed and mass action kinetics is followed. Thus, the glycolysis in a reaction region inside of a cell is represented by reaction network (2) and its corresponding dynamical ordinary differential equations are listed in (3).

$$\begin{array}{ll} S \rightleftarrows 0 \rightleftarrows M, & P \to 0, \\ S+E \rightleftarrows G+P, & S+T \rightleftarrows G+D, \\ G+T \rightleftarrows F+D, & F+2D \rightleftarrows 2E+2T, \\ E+D \rightleftarrows P+T, & M+T \rightleftarrows 2D, \\ D \rightleftarrows T. & \end{array} \tag{2}$$

$$\begin{aligned} \frac{\mathrm{d}c_M}{\mathrm{d}t} &= -k_{M\to 0}c_M + k_{0\to M} - k_{M+T\to 2D}c_M c_T \\ &\quad + k_{2D\to M+T}c_D^2, \\ \frac{\mathrm{d}c_S}{\mathrm{d}t} &= -k_{S\to 0}c_S + k_{0\to S} - k_{S+E\to G+P}c_S c_E \\ &\quad + k_{G+P\to S+E}c_G c_P - k_{S+T\to G+D}c_S c_T \\ &\quad + k_{G+D\to S+T}c_G c_D, \\ \frac{\mathrm{d}c_D}{\mathrm{d}t} &= 2k_{M+T\to 2D}c_M c_T - 2k_{2D\to M+T}c_D^2 - k_{D\to T}c_D \\ &\quad + k_{T\to D}c_T + k_{G+T\to F+D}c_G c_T \\ &\quad - k_{F+D\to G+T}c_F c_D - k_{E+D\to P+T}c_E c_D \\ &\quad + k_{P+T\to E+D}c_P c_T - 2k_{F+2D\to 2E+2T}c_F c_D^2 \\ &\quad + 2k_{2E+2T\to F+2D}c_E^2 c_T^2 + k_{S+T\to G+D}c_S c_T \\ &\quad - k_{G+D\to S+T}c_G c_D, \\ \frac{\mathrm{d}c_T}{\mathrm{d}t} &= -k_{M+T\to 2D}c_M c_T + k_{2D\to M+T}c_D^2 + k_{D\to T}c_D \\ &\quad - k_{T\to D}c_T - k_{G+T\to F+D}c_G c_T \\ &\quad + k_{F+D\to G+T}c_F c_D - k_{P+T\to E+D}c_P c_T \end{aligned}$$

$$
\begin{aligned}
&+ k_{E+D\to P+T}c_E c_D + 2k_{F+2D\to 2E+2T}c_F c_D^2 \\
&- 2k_{2E+2T\to F+2D}c_E^2 c_T^2 - k_{S+T\to G+D}c_S c_T \\
&+ k_{G+D\to S+T}c_G c_D, \\
\frac{\mathrm{d}c_G}{\mathrm{d}t} &= k_{S+E\to G+P}c_S c_E - k_{G+P\to S+E}c_G c_P \\
&- k_{G+T\to F+D}c_G c_T + k_{F+D\to G+T}c_F c_D \\
&+ k_{S+T\to G+D}c_S c_T - k_{G+D\to S+T}c_G c_D, \\
\frac{\mathrm{d}c_F}{\mathrm{d}t} &= k_{G+T\to F+D}c_G c_T - k_{F+D\to G+T}c_F c_D \\
&- k_{F+2D\to 2E+2T}c_F c_D^2 + k_{2E+2T\to F+2D}c_E^2 c_T^2, \\
\frac{\mathrm{d}c_E}{\mathrm{d}t} &= -k_{S+E\to G+P}c_S c_E + k_{G+P\to S+E}c_G c_P \\
&+ 2k_{F+2D\to 2E+2T}c_F c_D^2 - 2k_{2E+2T\to F+2D}c_E^2 c_T^2, \\
&- k_{E+D\to P+T}c_E c_D + k_{P+T\to E+D}c_P c_T, \\
\frac{\mathrm{d}c_P}{\mathrm{d}t} &= -k_{P\to 0}c_P + k_{S+E\to G+P}c_S c_E - k_{G+P\to S+E}c_G c_P \\
&- k_{P+T\to E+D}c_P c_T + k_{E+D\to P+T}c_E c_D, \qquad (3)
\end{aligned}
$$

where c_i $(i = M, S, \ldots, P)$ is denoting the concentrations of species $M, S, \ldots, P$ within the reactor and $k_{i\to j}$ is a rate constant for the reaction $i \to j$ in network (2).

The last seven lines in (2) are the elementary steps in the mechanism (1). The first two lines in (2) display the inflow of reactants and the outflow of remaining reactants and the products. In reaction network terms [17], to account for the inflow of M and S in the feed stream, the pseudo-reactions $0 \to M$ and $0 \to S$ are added to true chemistry (1). (The physical meaning of "0" (zero complex) represents the surroundings.) Compared with the dynamical equations in (3), the rate constants $k_{0\to M}$ and $k_{0\to S}$ are assigned respectively to be equal to c_M^f/θ and c_S^f/θ. (c_i^f denotes the feed concentration of species $i(= M, S)$ and θ denotes the residence time) Also, to account for the outflow of M, S and P in the effluent stream, pseudo-reactions $M \to 0$, $S \to 0$ and $P \to 0$ are added to true chemistry (1). The flow rates $k_{M\to 0}$, $k_{S\to 0}$ and $k_{P\to 0}$ are all assigned to be equal to the reciprocal of residence time θ. Thus, in reaction network terms, we consider the reactions given in (1), operating in an open system to be modeled by reaction network (2), instead of (1).

Example 2. Active membrane transport model

The example of the model 5 [14] is

$$
\begin{array}{ccc}
A_1 \rightleftarrows A_2 & & \\
\uparrow\downarrow \quad \uparrow\downarrow & A_3 + A_4 \rightleftarrows 2A_4 & \\
A_6 \quad A_3 & & \\
\uparrow\downarrow \quad \uparrow\downarrow & A_6 + A_7 \rightleftarrows A_8 \rightleftarrows A_1 + A_7 & \\
A_5 \rightleftarrows A_4 & &
\end{array} \qquad (4a)
$$

$$
\begin{aligned}
\frac{\mathrm{d}c_1}{\mathrm{d}t} &= -k_{A_1\to A_2}c_1 + k_{A_2\to A_1}c_2 - k_{A_1\to A_6}c_1 \\
&+ k_{A_6\to A_1}c_6 + k_{A_8\to A_1+A_7}c_8 - k_{A_1+A_7\to A_8}c_1 c_7, \\
\frac{\mathrm{d}c_2}{\mathrm{d}t} &= k_{A_1\to A_2}c_1 - k_{A_2\to A_1}c_2 \\
&- k_{A_2\to A_3}c_2 + k_{A_3\to A_2}c_3, \\
\frac{\mathrm{d}c_3}{\mathrm{d}t} &= k_{A_2\to A_3}c_2 - k_{A_3\to A_2}c_3 - k_{A_3\to A_4}c_3 \\
&+ k_{A_4\to A_3}c_4 + k_{2A_4\to A_3+A_4}c_4^2 - k_{A_3+A_4\to 2A_4}c_3 c_4, \\
\frac{\mathrm{d}c_4}{\mathrm{d}t} &= k_{A_3\to A_4}c_3 - k_{A_4\to A_3}c_4 + k_{A_3+A_4\to 2A_4}c_3 c_4 \\
&- k_{2A_4\to A_3+A_4}c_4^2 + k_{A_5\to A_4}c_5 - k_{A_4\to A_5}c_4, \\
\frac{\mathrm{d}c_5}{\mathrm{d}t} &= k_{A_4\to A_5}c_4 - k_{A_5\to A_4}c_5 \\
&- k_{A_5\to A_6}c_5 + k_{A_6\to A_5}c_6, \\
\frac{\mathrm{d}c_6}{\mathrm{d}t} &= k_{A_5\to A_6}c_5 - k_{A_6\to A_5}c_6 + k_{A_1\to A_6}c_1 \\
&- k_{A_6\to A_1}c_6 + k_{A_8\to A_6+A_7}c_8 - k_{A_6+A7\to A_8}c_6 c_7, \\
\frac{\mathrm{d}c_7}{\mathrm{d}t} &= -k_{A_6+A_7\to A_8}c_6 c_7 + k_{A_8\to A_6+A_7}c_8 \\
&+ k_{A_8\to A_1+A_7}c_8 - k_{A_1+A7\to A_8}c_1 c_7, \\
\frac{\mathrm{d}c_8}{\mathrm{d}t} &= -k_{A_8\to A_6+A_7}c_8 + k_{A_6+A_7\to A_8}c_6 c_7 \\
&- k_{A_8\to A_1+A_7}c_8 + k_{A_1+A7\to A_8}c_1 c_7, \qquad (4b)
\end{aligned}
$$

where c_i, $i = 1,2,\ldots,8$ denotes the concentrations of species $A_1, A_2, \ldots, A_8$ within the reactor, and $k_{i\to j}$ is a rate constant for the reaction $i \to j$ in network (4a).

Network (4a) contains one cycle $A_1 \to A_2 \to A_3 \to A_4 \to A_5 \to A_6 \to A_1$. During the cycle one ligand molecule is transported from the external to the internal medium. Each pump transports only one ion per cycle. The ligand concentration and the concentrations of ATP, ADP, and Pi (adenosine tri- and di-phosphate and inorganic phosphate, respectively) are considered as externally controlled parameters. Phosphorylation-dephosphorylation reactions and conformational transitions are treated as elementary steps. The autocatalytic reaction $A_3 + A_4 \rightleftarrows 2A_4$ comes from the fact that membranes of specialized cells of multicellular organisms and subcellular compartments of all eukaryotic cells have a restricted number of different proteins and usually a high concentration of each type, facilitating the interactions between them. The reactions $A_6 + A_7 \rightleftarrows A_8 \rightleftarrows A_1 + A_7$ model the formation of molecular complexes with other molecules, which should lead to activated monomers. From the kinetic point of view, the formation of an intermediate complex (A_8, pump-molecule) generates a new chemical pathway. A more detailed relation of network (4a) with reality is described by Vieira and Bisch in [14].

From network (4b), two mass conservation conditions must be satisfied. First, the sum of the concentrations of species A_7 and A_8 remains a constant. Second, the summation of concentrations of species A_1 through A_6 plus A_8 remains a constant. They must be satisfied by multiple steady states.

2.2. Deficiency One Algorithm and Subnetwork Analysis

In this paper the Deficiency One Algorithm [18] and the Subnetwork Analysis [16] are applied to determine the multiplicity of steady states in network (2), (4a) and their parent networks. In reaction network terms, each network has a deficiency, which is an integer equal to or greater than zero and can be calculated easily by the structure of a reaction network. Deficiency One Algorithm provides a necessary and sufficient condition for a deficiency one network to admit multiple steady states. By the analysis of this algorithm, the "signatures" of steady state multiplicity for a deficiency one reaction network are represented by many sets of linear inequality systems in terms of a vector $\boldsymbol{\mu}$. This vector $\boldsymbol{\mu}$ correlates two steady states, say c' and c'', corresponding to a set of rate constants in the following way:

$$\begin{aligned}\boldsymbol{\mu} &= [\mu_1,\ldots,\mu_N] \\ &\quad [\ln(c_1'/c_2''),\ldots,\ln(c_N'/c_N'')], \qquad (5)\\ N &= \text{ number of species.}\end{aligned}$$

If there exists such a nonzero $\boldsymbol{\mu}$ with the specified properties generated by the Deficiency One Algorithm, the deficiency one network under study has the capacity to admit multiple steady states. Otherwise, the network can admit at most one steady state.

The Deficiency One Algorithm is a powerful method to determine steady state multiplicity of a deficiency one-reaction network. However, there are some complex reaction networks lying outside the algorithm's applicable range. Take reaction network (2) and (4a), for examples. They both have a deficiency of two. Therefore, the Deficiency One Algorithm cannot be applied. The Subnetwork Analysis extends the applicable range of the algorithm by studying the subnetworks of a network with higher deficiency than one. Li [19] realized that networks of deficiency greater than one that admit multiple steady states often (not always) contain subnetworks that also have the capacity of exhibiting steady state multiplicity. An example has shown [19] that a parent network cannot admit multiple steady states, no matter what values the rate constants have, although one of its deficiency one subnetworks has the capacity to exhibit steady state multiplicity. Thus it is not trivial to ask the question: If a network contains a subnetwork that admits multiple steady states, under what conditions will the network also admit multiple steady states? The Subnetwork Analysis [16] provides sufficient conditions for the capacity of multiple steady states in a network of a deficiency greater than one if one of its subnetworks admits steady state multiplicity. (It can be applied to both forest-like and circular reaction networks.) The analysis is shown in the Appendix of this work, and the terminology and its implementation can be found in Li [16].

3. Results and Discussion

3.1. Bacterial Glycolysis Model

The procedure to determine multiple steady states of network (2) is to study its deficiency one subnetworks

by applying the Deficiency One Algorithm, to find a subnetwork admitting multiple steady states, and to apply the Subnetwork Analysis to determine the multiplicity of network (2). Moreover, the multiplicity is extended to some parent networks of the network (2) by using the Subnetwork Analysis.

According to the Deficiency One Algorithm, a deficiency one subnetwork of network (2) exhibiting multiple steady states is determined. It is obtained by deleting the fourth line of network (2) and displayed below.

$$\begin{array}{ll} S \rightleftarrows 0 \rightleftarrows M, & P \to 0, \\ S+E \rightleftarrows G+P, & G+T \rightleftarrows F+D, \\ F+2D \rightleftarrows 2E+2T, & E+D \rightleftarrows P+T, \\ M+T \rightleftarrows 2D, & D \rightleftarrows T. \end{array} \tag{6}$$

According to the algorithm, it has the capacity to admit multiple steady states if $\boldsymbol{\mu}$ defined in (5) satisfies the set of linear inequalities (7a) generated by the algorithm. It is easy to see that (7b) is a set of nonzero solutions to (7a). (7a) indicates the relationships of the two steady states, which can be used to identify the mechanism if the steady states of some species are measured. The more inequalities and (7a) are satisfied by the experimental data, the more likely the mechanism (6) is followed. (The reverse of all the inequalities (7a) is also a signature of multiple steady states, which is obtained by exchanging c' and c'' (5).)

$$\begin{array}{rcl} \boldsymbol{\mu}_M & < & \boldsymbol{\mu}_P \\ \boldsymbol{\mu}_T & < & \boldsymbol{\mu}_P \\ \boldsymbol{\mu}_S & < & 0 \\ \boldsymbol{\mu}_D & < & \boldsymbol{\mu}_T \\ \boldsymbol{\mu}_P & < & \boldsymbol{\mu}_S+\boldsymbol{\mu}_E \\ \boldsymbol{\mu}_S+\boldsymbol{\mu}_E & < & \boldsymbol{\mu}_P+\boldsymbol{\mu}_G \\ \boldsymbol{\mu}_P & < & \boldsymbol{\mu}_T+\boldsymbol{\mu}_G \\ \boldsymbol{\mu}_T+\boldsymbol{\mu}_G & < & \boldsymbol{\mu}_D+\boldsymbol{\mu}_F \\ \boldsymbol{\mu}_P & < & 2\boldsymbol{\mu}_D+\boldsymbol{\mu}_F \\ 2\boldsymbol{\mu}_D+\boldsymbol{\mu}_F & < & 2\boldsymbol{\mu}_T+2\boldsymbol{\mu}_E \\ \boldsymbol{\mu}_P & < & \boldsymbol{\mu}_D+\boldsymbol{\mu}_E \\ \boldsymbol{\mu}_D+\boldsymbol{\mu}_E & < & \boldsymbol{\mu}_P+\boldsymbol{\mu}_T \\ \boldsymbol{\mu}_M & = & 0 \\ \boldsymbol{\mu}_M+\boldsymbol{\mu}_T & = & 2\boldsymbol{\mu}_D \end{array} \tag{7a}$$

$$\begin{aligned} \boldsymbol{\mu} &= [\mu_M, \mu_S, \mu_D, \mu_T, \mu_G, \mu_F, \mu_E, \mu_P,] \\ &= [0,-1,3,6,2,6,9,7] \end{aligned} \tag{7b}$$

By the $\boldsymbol{\mu}$ given in (7b), a set of rate constants, displayed in (8a), and its two corresponding steady states, c' and c'' in (8b), are computed. (The formulas for the computation of two steady states and a set of rate constants can be found in Feinberg [18].)

$$\begin{array}{ll} S \underset{1734.27}{\overset{1095.63}{\rightleftarrows}} 0 \underset{1095.63}{\overset{1095.63}{\rightleftarrows}} M, & P \xrightarrow{1095.63} 0, \\ S+E \underset{429.20}{\overset{2335.20}{\rightleftarrows}} G+P, & G+T \underset{313.95}{\overset{390.78}{\rightleftarrows}} F+D, \\ F+2D \underset{1985.41}{\overset{5429.18}{\rightleftarrows}} 2E+2T, & E+D \underset{42478.82}{\overset{27113.20}{\rightleftarrows}} P+T, \\ M+T \underset{40.47}{\overset{134.14}{\rightleftarrows}} 2D, & D \underset{753.43}{\overset{23.01}{\rightleftarrows}} T. \end{array} \tag{8a}$$

$$\begin{array}{ll} c'_M \approx 1.000000, & C''_M \approx 1.000000, \\ c'_S \approx 0.581977\,, & C''_S \approx 1.581977, \\ c'_D \approx 3.157187\,, & C''_D \approx 0.157187, \\ c'_T \approx 3.007455\,, & C''_T \approx 0.007455, \\ c'_G \approx 3.469553\,, & C''_G \approx 0.469553, \\ c'_F \approx 3.007455\,, & C''_F \approx 0.007455, \\ c'_E \approx 3.000370\,, & C''_E \approx 0.000370, \\ c'_P \approx 2.001825\,, & C''_P \approx 0.001825. \end{array} \tag{8b}$$

In Fig. 1, the steady states and bistability occurring in network (8) are illustrated as hysteresis with variation of $k_{0\to S}$. The steady states c'_P (the upper points in Fig. 1) and c''_P (the lower points in Fig. 1) in (8b) are stable and an unstable steady state (not shown in Fig. 1) lies somewhere between c' and c''. The steady state c'' in (8b) established at a lower $k_{0\to S}$ (< 893) is associated with a lower concentrations c_P. As $k_{0\to S}$ is higher than 2011, the steady state associating with a higher concentration c_P is obtained. As $k_{0\to S}$ is in between, a hysteresis loop containing three steady states, two stable ones and an unstable one, occurs and the steady state depends on the initial concentrations. Figure 2 shows a similar hysteresis loop with variation of $k_{S\to 0}$ (= flow rate) in the range of $971 < k_{S\to 0} < 2008$.

Figure 3 shows a two-parameter ($k_{M+T\to 2D}$, $k_{0\to S}$) plane for different values of the rate constant $k_{G+T\to F+D}$ for network (8). (The solid line corresponds to 390.78 and the dotted line to 1187, respectively.) Inside the cusp regions, there are three steady states, two stable ones and an unstable one. They display the inside regions of a hysteresis loop similar to Figs. 1 and 2. Right on the curves of the cusp, there are two steady states, a stable one and an unstable one. They represent the two end points of a hysteresis loop. Only a single steady state exists outside the cusp region in Fig. 3, which displays the outside region of a hysteresis loop.

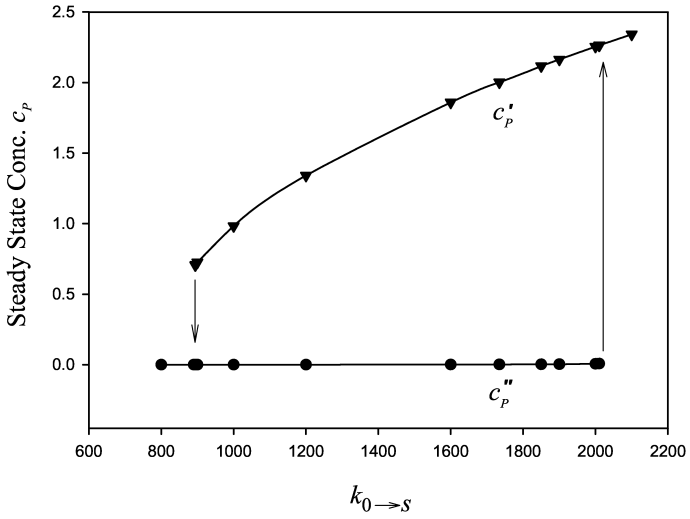

Fig. 1. The change of the steady state concentration c_P with the rate constant $k_{0\to S}$ for network (8).

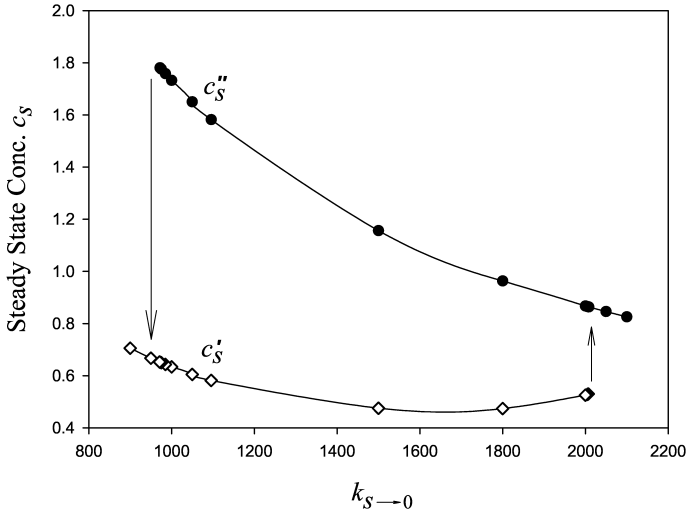

Fig. 2. The change of the steady state concentration c_S with the flow rate $k_{S\to 0}$ for network (8).

Note the equality of the rate constants in (8a) calculated for the pseudo-reactions $M \to 0$, $S \to 0$, and $P \to 0$. As mentioned before, their corresponding rate constants should all be equal to the flow rate. Thus, equality of the flow rate $k_{M\to 0}$, $k_{S\to 0}$, and $k_{P\to 0}$, in the reaction network (8a) is consistent with the picture of a flow system.

According to the Subnetwork Analysis, the network (2) also has the capacity to admit multiple steady states for the vector $\boldsymbol{\mu}$ given in (7). The rate constants and corresponding two steady states are indicated in (9), computing according to the vector $\boldsymbol{\mu}$ given in (7b). (The formulas for the computation of two steady states and a set of rate constants can be found in the appendix of [20].) Figure 4 shows a two-parameter ($k_{S+T\to G+D}$, $k_{0\to S}$) plane for different values of the rate constant $k_{G+T\to F+D}$ of network (9). (The solid line corresponds to 390.78 and the dotted line to 800, respectively.) Inside the cusp regions, there are three steady states, two stable ones and an unstable one. Only a single steady state exists outside the cusp region in Figure 4.

$$S \underset{1734.27}{\overset{1095.63}{\rightleftarrows}} 0 \underset{1095.63}{\overset{1095.63}{\rightleftarrows}} M, \quad P \xrightarrow{1095.63} 0,$$

$$S + E \underset{106.61}{\overset{1009.58}{\rightleftarrows}} G + P, \quad G + T \underset{313.95}{\overset{390.78}{\rightleftarrows}} F + D,$$

$$F + 2D \underset{1985.41}{\overset{5429.18}{\rightleftarrows}} 2E + 2T, \quad E + D \underset{63842.81}{\overset{40698.93}{\rightleftarrows}} P + T,$$

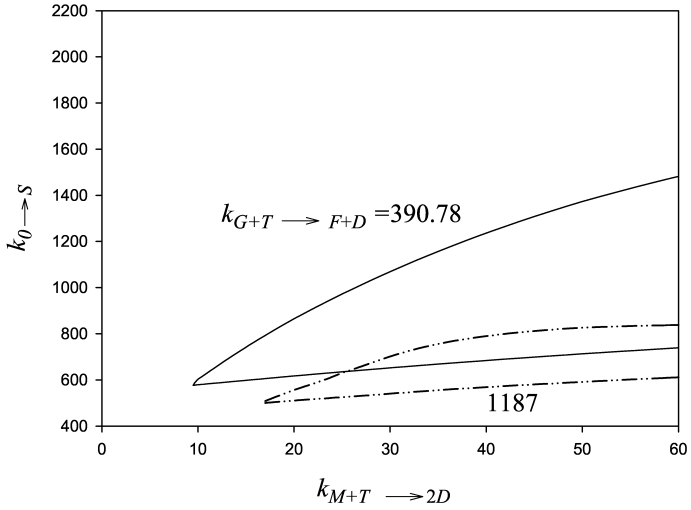

Fig. 3. The locus of the multiple steady state bifurcation for network (8) in the ($k_{M+T\to 2D}$, $k_{0\to S}$) plane for different values of the rate constant $k_{G+T\to F+D}$. Inside the cusp regions there are three steady states, two stable ones and an unstable one. Only a single steady state exists outside.

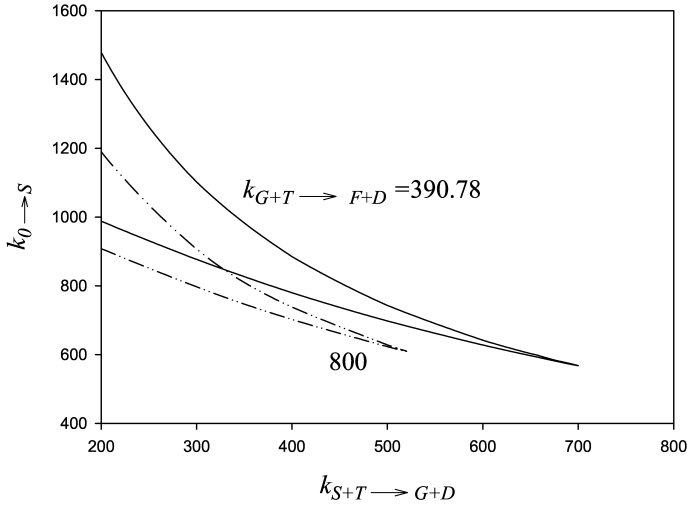

Fig. 4. The locus of multiple steady state bifurcation for network (9) in the ($k_{S+T\to G+D}$, $k_{0\to S}$) plane for different values of the rate constant $k_{G+T\to F+D}$. Inside the cusp regions there are three steady states, two stable ones and an unstable one. Only a single steady state exists outside.

$$M+T \underset{40.47}{\overset{134.14}{\rightleftarrows}} 2D, \quad D \underset{753.43}{\overset{23.01}{\rightleftarrows}} T,$$
$$S+T \underset{13.55}{\overset{127.19}{\rightleftarrows}} G+D. \tag{9a}$$

$$\begin{aligned}
c'_M &\approx 1.000000, & C''_M &\approx 1.000000,\\
c'_S &\approx 0.581977, & C''_S &\approx 1.581977,\\
c'_D &\approx 3.157187, & C''_D &\approx 0.157187,\\
c'_T &\approx 3.007455, & C''_T &\approx 0.007455,\\
c'_G &\approx 3.469553, & C''_G &\approx 0.469553,\\
c'_F &\approx 3.007455, & C''_F &\approx 0.007455,\\
c'_E &\approx 3.000370, & C''_E &\approx 0.000370,\\
c'_P &\approx 2.001825, & C''_P &\approx 0.001825.
\end{aligned} \tag{9b}$$

The addition of a pair of the reversible reaction $S+2T \rightleftarrows F+2D$ to network (2) leads to the network (10) of deficiency three. Following the Subnetwork Analysis, the augmented network also has the capacity to admit multiple steady states. The rate constants in (10) and corresponding two steady states (11) are computed by using the vector $\boldsymbol{\mu}$ given in (7b). Figure 5 shows a two-parameter ($k_{S+2T\to F+2D}$, $k_{0\to S}$) plane for different values of the rate constant $k_{G+T\to F+D}$ for network (10). (The solid line corresponds to 362.21 and the dotted line to 750, respectively.) Although the lower points on the dotted line nearly overlap those on the solid line, it is similar to Figure 4.

$$S \underset{1734.27}{\overset{1095.63}{\rightleftarrows}} 0 \underset{1095.63}{\overset{1095.63}{\rightleftarrows}} M, \quad P \xrightarrow{1095.63} 0,$$
$$S+E \underset{106.61}{\overset{1009.58}{\rightleftarrows}} G+P, \quad G+T \underset{313.95}{\overset{362.21}{\rightleftarrows}} F+D,$$

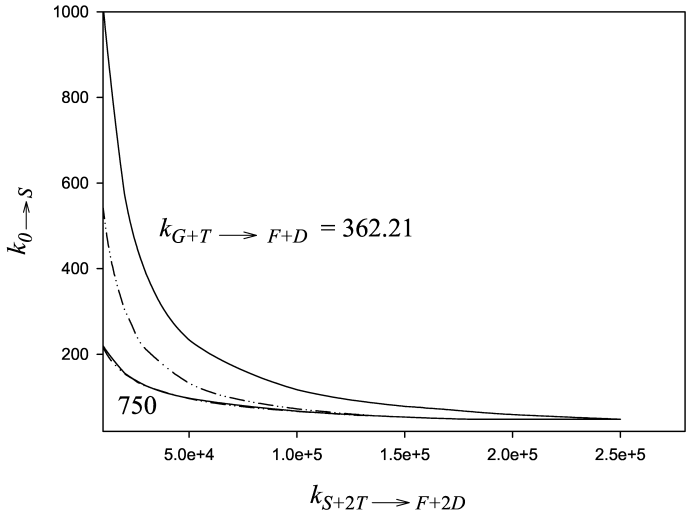

Fig. 5. The locus of multiple steady state bifurcation for network (10) in the ($k_{S+2T\to F+2D}$, $k_{0\to S}$) plane for different values of the rate constant $k_{G+T\to F+D}$. Inside the cusp regions there are three steady states, two stable ones and an unstable one. Only a single steady state exists outside.

$$
\begin{aligned}
&E+D \underset{63842.81}{\overset{40698.93}{\rightleftarrows}} P+T, \quad M+T \underset{40.47}{\overset{134.14}{\rightleftarrows}} 2D,\\
&D \underset{753.43}{\overset{23.01}{\rightleftarrows}} T, \quad S+T \underset{13.55}{\overset{118.71}{\rightleftarrows}} G+D,\\
&S+2T \underset{300.23}{\overset{1766.47}{\rightleftarrows}} F+2D \underset{1985.41}{\overset{5429.18}{\rightleftarrows}} 2E+2T.
\end{aligned} \tag{10}
$$

$$
\begin{aligned}
&c'_M \approx 1.000000, \quad C''_M \approx 1.000000,\\
&c'_S \approx 0.581977\,, \quad C''_S \approx 1.581977,\\
&c'_D \approx 3.157187\,, \quad C''_D \approx 0.157187,\\
&c'_T \approx 3.007455\,, \quad C''_T \approx 0.007455,\\
&c'_G \approx 3.469553\,, \quad C''_G \approx 0.469553,\\
&c'_F \approx 3.007455\,, \quad C''_F \approx 0.007455,\\
&c'_E \approx 3.000370\,, \quad C''_E \approx 0.000370,\\
&c'_P \approx 2.001825\,, \quad C''_P \approx 0.001825.
\end{aligned} \tag{11}
$$

Following the Subnetwork Analysis, the family members of subnetwork (6) displayed in network (12) have the capacity to exhibit multiple steady states for the vector $\boldsymbol{\mu}$ in (7). The first eight lines of network (12) are just the deficiency one subnetwork (6). The parameters a, b, c, …, f in the last line of network (12) are any real numbers. A negative parameter means the reverse of the reaction arrow. The last line of reaction network (12) describes any of the reactions which can be represented by a linear combination of those reactions on the right-hand side of the equation. The network (12) might have high deficiency, such as network (9) of deficiency two, network (10) of deficiency three, and even other networks of higher deficiency.

$$
\begin{aligned}
&S \rightleftarrows 0 \rightleftarrows M, && P \to 0,\\
&S+E \rightleftarrows G+P, && G+T \rightleftarrows F+D,\\
&F+2D \rightleftarrows 2E+2T, && E+D \rightleftarrows P+T,\\
&M+T \rightleftarrows 2D, && D \rightleftarrows T,
\end{aligned} \tag{12}
$$

$$
\begin{aligned}
y_i \to y_j = {} & a(S\to 0) + b(S+E\to G+P)\\
& + c(G+T\to F+D)\\
& + d(F+2D\to 2E+2T)\\
& + e(E+D\to P+T) + f(D\to T).
\end{aligned}
$$

3.2. Active Membrane Transport Model

Since the reaction network (4a) has deficiency two, the Deficiency One Algorithm cannot be applied directly. Analyzing subnetworks of network (4a) by the algorithm, we find that the deficiency one subnetwork (13a), obtained from parent network (4a) by deleting reactions $A_1 \rightleftarrows A_6$ and $A_3 \rightleftarrows A_4$, can exhibit steady state multiplicity. For the rate constants shown in network (13a), it exhibits two steady states c' and c'' in (13b).

$$
\begin{aligned}
&A_1 \underset{0.4435}{\overset{0.6535}{\rightleftarrows}} A_2 \underset{0.2615}{\overset{0.3410}{\rightleftarrows}} A_3, \quad A_4 \underset{0.1915}{\overset{0.2429}{\rightleftarrows}} A_5 \underset{0.3674}{\overset{0.4188}{\rightleftarrows}} A_6,\\
&A_3 + A_4 \underset{0.0003}{\overset{0.0023}{\rightleftarrows}} 2A_4,\\
&A_6 + A_7 \underset{0.0669}{\overset{0.1777}{\rightleftarrows}} A_8 \underset{0.0080}{\overset{0.2732}{\rightleftarrows}} A_1 + A_7,
\end{aligned} \tag{13a}
$$

$$\begin{aligned}
&c_1' \approx 25.2200, \quad C_1'' \approx 22.8200,\\
&c_2' \approx 35.3733, \quad C_2'' \approx 31.3733,\\
&c_3' \approx 43.0750, \quad C_3'' \approx 37.0750,\\
&c_4' \approx 8.1330\ , \quad C_4'' \approx 12.1330,\\
&c_5' \approx 6.1660\ , \quad C_5'' \approx 10.1660,\\
&c_6' \approx 4.8655\ , \quad C_6'' \approx 8.8655,\\
&c_7' \approx 1.2133\ , \quad C_7'' \approx 0.8133,\\
&c_8' \approx 3.8033\ , \quad C_8'' \approx 4.2033.
\end{aligned} \tag{13b}$$

Moreover, the deficiency one algorithm indicates that network (13a) admits multiple steady states if and only if the vector $\boldsymbol{\mu}$ defined in (5) satisfies (14a) and a mass conversation requirement: the elements of the sets $[\mu_7, \mu_8]$ and $[\mu_1, \ldots, \mu_6, \mu_8]$ contain both a positive and negative number, or else consists entirely of zeros. The $\boldsymbol{\mu}$ listed in (14b) is a qualified solution. This constraint can be used to identify the mechanism if steady states of some species are measured by experiments.

$$\left\{ \begin{array}{c} \mu_3 > \mu_2 > \mu_1 \\ \mu_1 + \mu_7 > \mu_8 > \mu_6 + \mu_7 \end{array} \right\} > \left\{ \begin{array}{l} \mu_4 > \mu_5 > \mu_6 \\ \mu_3 + \mu_4 > 2\mu_4 \end{array} \right\}. \tag{14a}$$

$$\begin{aligned}
&\boldsymbol{\mu}[\mu_1, \mu_2, \ldots, \mu_8]\\
&\quad = [0.1, 0.12, 0.15, -0.4, -0.5, -0.6, 0.4, -0.1].
\end{aligned} \tag{14b}$$

We can generalize the capacity of multiple steady states to the family members of network (13a) according to the Subnetwork Analysis. Let network (13a) be a base subnetwork. The multiplicity of steady states remains for the augmented parent networks, as long as the reaction vectors of the added reactions can be represented as a linear combination of any reaction vectors of network (13a). This family reaction network is shown in (15), where the parameter x_i can be any real number. A negative parameter means the reverse of the reaction arrow. The reactions given in (16) are some examples of the reactions which can be added to the subnetwork (13a). The reaction network (4a) of deficiency two is such an example.

$$\begin{aligned}
&A_1 \rightleftarrows A_2 \rightleftarrows A_3,\\
&A_4 \rightleftarrows A_5 \rightleftarrows A_6,\\
&A_3 + A_4 \rightleftarrows 2A_4, \quad A_6 + A_7 \rightleftarrows A_8 \rightleftarrows A_1 + A_7,\\
&y_1 \to y_j = x_1(A_1 \to A_2) + x_2(A_2 \to A_3)\\
&\qquad + x_3(A_4 \to A_5) + x_4(A_5 \to A_6)\\
&\qquad + x_5(A_3 + A_4 \to 2A_4)\\
&\qquad + x_6(A_6 + A_7 \to A_8)\\
&\qquad + x_7(A_8 \to A_1 + A_7).
\end{aligned} \tag{15b}$$

$$aA_i \Leftrightarrow aA_j, \quad i = 1, \ldots, 4, \quad j = i+2, \ldots, 6, \tag{16a}$$

$$bA_i + cA_j \Leftrightarrow (b+c)A_k, \quad i, j, k = 1, \ldots, 6, \tag{16b}$$

$$dA_8 \Leftrightarrow dA_7 + dA_i, \quad i = 1, \ldots, 6, \tag{16c}$$

$$\begin{aligned}
&eA_i + fA_7 + gA_8 \Leftrightarrow eA_j + fA_7 + gA_8,\\
&i, j = 1, \ldots, 6,
\end{aligned} \tag{16d}$$

(a, b, …, g are any non-negative real numbers, and the symbol "$\Leftrightarrow$" means either "$\to$", "$\leftarrow$", or "$\rightleftarrows$".)

Network (17a) of deficiency five is a combination of network (13a) and (16), which is a parent network of the network (4) of deficiency two. It has the capacity to admit two steady states in (17b), which satisfy (14b) and the mass conservation condition. Many other possible combinations of parent networks also admit multiple steady states.

$$\begin{aligned}
&A_1 \underset{38.1703}{\overset{56.4211}{\rightleftarrows}} A_2,\\
&A_2 \underset{23.0226}{\overset{30.0912}{\rightleftarrows}} A_3,\\
&A_3 \underset{0.3141}{\overset{0.0758}{\rightleftarrows}} A_4, \quad A_3 + A_4 \underset{0.0065}{\overset{0.2033}{\rightleftarrows}} 2A_4 \underset{0.0030}{\overset{0.0099}{\rightleftarrows}} A_2 + A_5,\\
&A_4 \underset{17.9848}{\overset{22.5281}{\rightleftarrows}} A_5, \quad A_6 + A_7 \underset{4.0313}{\overset{14.8323}{\rightleftarrows}} A_8 \underset{0.6015}{\overset{23.8294}{\rightleftarrows}} A_1 + A_7,\\
&A_5 \underset{33.4810}{\overset{38.1493}{\rightleftarrows}} A_6, \quad A_8 \underset{0.9636}{\overset{2.5000}{\rightleftarrows}} A_4 + A_7,\\
&A_6 \underset{0.0036}{\overset{0.1221}{\rightleftarrows}} A_1, \quad A_6 + A_7 \xrightarrow{0.1387} A_4 + A_7,\\
&A_3 \underset{0.0110}{\overset{0.0296}{\rightleftarrows}} A_6.
\end{aligned} \tag{17a}$$

$$\begin{aligned}
&c_1' \approx 25.2200, \quad C_1'' \approx 22.8200,\\
&c_2' \approx 35.3733, \quad C_2'' \approx 31.3733,\\
&c_3' \approx 43.0750, \quad C_3'' \approx 37.0750,\\
&c_4' \approx 8.1330\ , \quad C_4'' \approx 12.1330,\\
&c_5' \approx 6.1660\ , \quad C_5'' \approx 10.1660,\\
&c_6' \approx 4.8655\ , \quad C_6'' \approx 8.8655,\\
&c_7' \approx 1.2133\ , \quad C_7'' \approx 0.8133,\\
&c_8' \approx 3.8033\ , \quad C_8'' \approx 4.2033.
\end{aligned} \tag{17b}$$

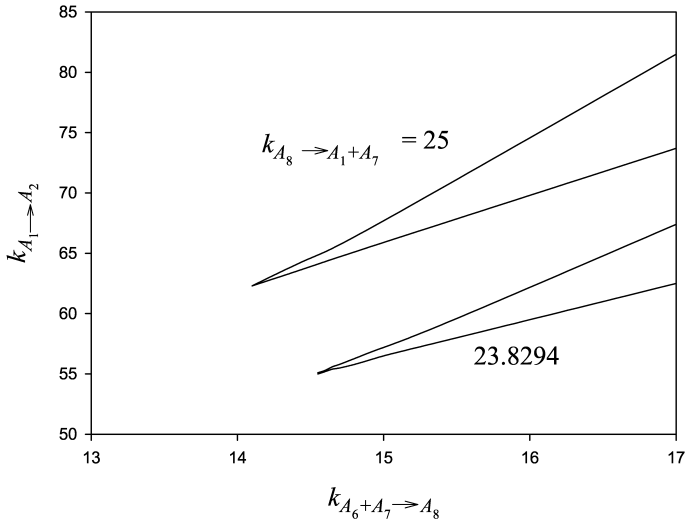

Fig. 6. The locus of the multiple steady state bifurcation for network (17) in the ($k_{A_6+A_7\to A_8}$, $k_{A_1\to A_2}$) plane for different values of rate constant $k_{A_8\to A_1+A_7}$. Inside the cusp regions there are three steady states, two stable ones and an unstable one. Only a single steady state exists outside.

Numerical analysis is simulated for the system (17). Figure 6 shows a two-parameter ($k_{A_6+A_7\to A_8}$, $k_{A_1\to A_2}$) multiplicity bifurcation diagram of network (17) for different values of $k_{A_8\to A_1+A_7}$. Figure 6 shows that, to maintain the existence of the steady state multiplicity under a fixed rate constant $k_{A_6+A_7\to A_8}$, the larger the rate constant $k_{A_8\to A_1+A_7}$ is, the larger the rate constant $k_{A_1\to A_2}$ is required and the wider the range in which it exists. To maintain the existence of the steady state multiplicity under a lower rate constant $k_{A_6+A_7\to A_8}$, it is required to reduce the rate constant $k_{A_1\to A_2}$ for a fixed rate constant $k_{A_8\to A_1+A_7}$.

The nonlinear dynamics approach, introduced by Kuramoto [21], can be applied to the dynamics of self-oscillating fields of the reaction-diffusion type and some related systems. Such systems, forming cooperative fields of a large number of interacting similar subunits, are considered as typical synergetic systems. In some cases, the total system can be viewed as an assembly of a large number of identical local systems which are diffusion-coupled to each other. The local system obeys a set of ordinary differential equations which are first order in time. The methods used are the reductive perturbation method, and the phase description method. Our approach in this work deals with a set of ordinary differential equations first order in time, which is suitable for the analysis of the subunits of the whole reaction-diffusion system. Moreover, our approach can apply to systems of many variables coupled with many non-linear equations, which may become much cumbersome when solved by the perturbation method. Therefore, as a complex reaction system is determined to admit multiple steady states by our method, it can be viewed as a subunit and be applied by Kuramoto's approach to study the nonlinear dynamics of the whole reaction-diffusion system. Or our method can be applied directly to the reaction-convection system, which involves only ordinary differential equations first order in time, such as multicell reaction systems [22, 23].

4. Conclusion

The Subnetwork Analysis is used to determine the capacity of multiple steady states for two families of complex biochemical reaction networks (12) and (15). The bistability, hysteresis and bifurcation phenomena are discussed. The inequalities and equations listed in (7a) and (14a) provide signatures of steady state multiplicity for their families of networks, which can be used to identify reaction mechanism if steady states of some species are measured. The results of this work might help to study the complex reaction networks in other biological systems. From a metabolic engineering point of view, it can be also applied to investigate glycolysis in other organisms, such as mammalian cells and yeast, even though they have different stoichiometry. At the course of breakdown of glucose to obtain energy in cells, this work mainly focuses on glycolysis. An oxidative catabolism system, which couples a glycolysis model, a citrical acid cycle and a respiratory chain are currently under investigation. It involves not only the ATP generation from glucose but also the conversion of pyruvate to carbon dioxide and

water. The results of this work serve as a guide to such complex reaction networks.

Appendix

Subnetwork Analysis: *Consider a network Q, $\{Z_Q, C_Q, R_Q\}$. Let A, $\{Z_A, C_A, R_A$ be a subnetwork of Q such that*

(i) $Z_A = Z_Q$.

(ii) $y_j \to y_i \notin R_Q \backslash R_A$, $\forall y_i \to y_j \in R_A$.

(iii) *Subnetwork A admits multiple steady states c' and c''.*

(iv) $y_j - y_i \in sR_a^{\neq}(\boldsymbol{\mu})$, $\forall y_i \to y_j \in R_Q \backslash R_A$.

Then network Q admits multiple steady states for the $\boldsymbol{\mu}$ computed by c' and c''. (It is defined that $R_Q \backslash R_A$ is the set consisting of reactions in R_Q but not in R_A.)

[1] I. Epelboin, M. Ksouri, and R. J. Wiart, J. Electrochem. Soc. **122**, 1206 (1972).
[2] W. Geiseler and K. Bar-Eli, J. Phys. Chem. **85**, 908 (1981).
[3] M. Orbán and I. R. Epstein, J. Amer. Chem. Soc. **107**, 2302 (1985).
[4] A. K. Dutt and S. C. Müller, J. Chem. Phys. **104**, 583 (1996).
[5] J. E. Bailey, Biotechnol. Prog. **14**, 8 (1998).
[6] H.-Y. Li, J. Chem. Phys. **109**, 8485 (1998).
[7] F. Hynne, S. Danø, and P. G. Sørensen, Biophysical Chemistry **94**, 121 (2001).
[8] G. Gottschalk, Bacterial Metabolism, 2nd Edn., Springer, New York 1986.
[9] V. Hatzimanikatis and J. E. Bailey, Chem. Eng. Sci. **52**, 2579 (1997).
[10] C. Tanford, Annu. Rev. Biochem. **52**, 379 (1983).
[11] A. Goldbeter, G. Dupont, and M. J. Berridge, Proc. Nacl. Acad. Sci. USA **87**, 1461 (1990).
[12] A. T. Tepikin, S. G. Voronin, D. V. Gallacher, and O. H. Petersen, J. Biol. Chem. **267**, 14073 (1992).
[13] D. Kosk-Kosicka and T. Bzdega, Biochemistry. **29**, 3772 (1990).
[14] F. M. C. Vieira and P. M. Bisch, Eur. Biophys. J. **23**, 277 (1994).
[15] B. L. Clarke, Adv. Chem. Phys. **43**, 1 (1980).
[16] H.-Y. Li, Chem. Eng. Sci. **53**, 3703 (1998).
[17] M. Feinberg, Chem. Eng. Sci. **42**, 2229 (1987).
[18] M. Feinberg, Chem. Eng. Sci. **43**, 1 (1988).
[19] H.-Y. Li, Ph.D. Dissertation, University of Rochester, NY 1992.
[20] H.-Y. Li, Z. Naturforsch. **54a**, 245 (1999).
[21] Y. Kuramoto, Chemical Oscillations, Waves, and Turbulence. Chapts. 6 – 7, Springer-Verlag, Tokyo 1984.
[22] A. Shapiro and F. J. M. Horn, Mathematical Biosciences. **44**, 19 (1979).
[23] M. Korc, Ph.D. Dissertation, University of Rochester, NY 1992.